PAPER

Evidence of strong O−H···C interactions involving apical pyramidane carbon atoms as hydrogen atom acceptors†

Ivana S. Veljković, [iD] [a] Miroslavka Malinić[b] and Dušan Ž. Veljković [iD] *[b]

Using high-level quantum chemical calculations, we predicted a strong O−H···C interaction between the apical carbon atoms of pyramidane and its derivatives and water molecules. Analysis of calculated electrostatic potential maps showed that there are areas of strong negative potential above apical carbon atoms in all studied structures. The results of quantum chemical calculations showed that the O−H···C interaction between the hydrogen atom of water and the apical carbon atom of pyramidane derivatives with four −CH$_3$ substituents is unexpectedly strong, $\Delta E_{\text{CCSD(T)/CBS}}$ = −7.43 kcal mol^{-1}. The strong hydrogen bonds were also predicted in the case of unsubstituted pyramidane ($\Delta E_{\text{CCSD(T)/CBS}}$ = −6.41 kcal mol^{-1}) and pyramidane with four −OH substituents ($\Delta E_{\text{CCSD(T)/CBS}}$ = −5.87 kcal mol^{-1}). Although there are not many crystal structures of pyramidane-like molecules, we extracted examples of pyramidal-shaped molecules with apical carbon atoms from the Cambridge Structural Database and analyzed their hydrogen-bonding patterns. Analysis of crystal structures confirmed the existence of short non-covalent contacts between apical carbon atoms and neighboring hydrogen atoms.

Introduction

Hydrogen bonds play a crucial role in numerous chemical, physical, and biological phenomena and processes.[1–9] According to an IUPAC definition, a hydrogen bond (depicted as D–H···A) is formed between a hydrogen atom bonded to an electronegative atom (donor atom, D) and another electron-rich atom (acceptor atom, A).[10] In more general terms, the acceptor does not have to be an electron-rich atom but could be any species with increased electron density (including aromatic systems, π-bonds, radicals, *etc.*). Along these lines, in addition to usual hydrogen atom acceptors like O, N, or F atoms, there is a possibility that other atoms may play that role, too. This was discussed in detail in a very recent review on specific types of hydrogen bonds.[11] One of the unexpected candidates for the role of hydrogen atom acceptor is the carbon atom.[11–14] Although electron-rich carbon atoms are not usual in molecules, there are indeed examples of organic and organometallic compounds in which an increased electron density is detected around the C atom. An early example of a non-covalent carbon-hydrogen contact was noticed in the crystal structure of the carbene complex.[12] The C–H···C bond between two carbene moieties was analysed in terms of geometry, and the analysis showed that the C–H···C angle is almost linear (172.5°), which is the characteristic of hydrogen bonds. Also, the distance between interacting C and H atoms (2.02 Å) was shorter than the sum of their van der Waals radii, indicating the existence of a hydrogen bond. In the very recent study performed by S. Grabowski, C–H$^+$···C hydrogen bonds between carbon atoms of N-heterocyclic carbenes (NHC) and a proton of a hydrogen-containing cation were detected in crystal structures extracted from the Cambridge Structural Database (CSD).[14] The results of density functional theory (DFT) calculations performed at the BP86-D4/TZ2P level showed that these interactions may be quite strong, as expected for charged species like cations.[14]

Another theoretical study showed that carbenes may also be involved in X–H···C interactions with neutral species.[13] *Ab initio* calculations performed at the MP2/aug-cc-pVTZ level showed that carbenes and carbodiphosphoranes may be involved in X–H···C interactions (X = O, C) in which divalent carbon atoms act as hydrogen atom acceptors.[13] The results of quantum chemical calculations indicate that a strong O–H···C interaction may be formed between imidazole-2-ylidene and a water molecule (ΔE = −9.84 kcal mol^{-1}). These unusual properties of carbon atoms were explained by the presence of lone pairs on C atoms in these specific systems. Examples of unusual X–H···C interactions involving carbon atoms of a methyl group as hydrogen atom acceptors were recognized in crystal structures, too.[15]

[a] University of Belgrade – Institute of Chemistry, Technology and Metallurgy – National Institute of the Republic of Serbia, Belgrade, Serbia

[b] University of Belgrade – Faculty of Chemistry, Studentski trg 12-16, Belgrade, Serbia. E-mail: vdusan@chem.bg.ac.rs

† Electronic supplementary information (ESI) available. See DOI: https://doi.org/10.1039/d4cp03809f

This journal is © the Owner Societies 2025

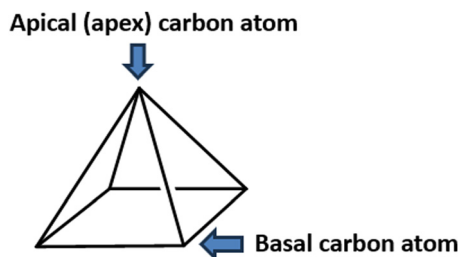*Phys. Chem. Chem. Phys.*, 2025, **27**, 2563–2569 | **2563**

Fig. 1 The structure of a pyramidane molecule. The carbon atom on the top of the pyramidal structure is designated as an "apical" or an "apex" carbon atom, while other carbon atoms are designated as "basal" carbon atoms.

Pyramidane (tetracyclo[2.1.0.0^{1,3},2.0^{3,5}]pentane) is a hydrocarbon molecule with a pyramidal-shape structure (Fig. 1).[16] Due to its unusual bonding characteristics, possible application as a high-energy material precursor, and the fact that it has never been synthesized, the pyramidane molecule has attracted significant attention from both theoretical and synthetic chemists.[16–22] However, many heteroatom pyramidane analogs were synthesized and structurally characterized, including both charged and neutral chemical species.[17–20]

Combined experimental and theoretical studies indicate the presence of non-classical bonding in the pyramidane molecule and its derivatives, with a high degree of ionicity of the bonds between apical and basal carbon atoms.[21] The results of DFT calculations show that an electron pair with a very high s character exists at the apex of the pyramidal structure.[21] These results indicate that the apical carbon atoms in the pyramidane molecule and its derivatives may act as hydrogen atom acceptors in hydrogen bonds. Furthermore, calculations performed within the same study showed that the nature of substituents on basal carbon atoms significantly affects the structure and bonding in pyramidal molecules, which may also have consequences in terms of non-covalent bonding patterns.

Although covalent bonding in pyramidane and many of its derivatives was extensively studied in the past, a systematic study of non-covalent interactions involving these molecules has not been performed yet. On the other hand, it is known that in the case of some strained high-energy molecules, hydrogen bonds play very important roles in terms of their detonation properties.[22] DFT calculations performed on a series of nitrocyclohydrocarbon explosives showed that hydrogen bonding affects the sensitivity of these molecules towards detonation.[22]

In this study, we have performed high-level *ab initio* calculations to predict and characterize possible O–H···C interactions involving the apical carbon atom of pyramidane and substituted pyramidane molecules as hydrogen atom acceptors. We also studied the influence of substituents attached to base carbon atoms on the properties of hydrogen bonds involving apical carbon atoms.

Methodology

All geometry optimizations, vibrational spectra, wave function files, and interaction energy calculations performed within this study were performed using the Gaussian09[23] software package

and the MP2 method[24] combined with the aug-cc-pVTZ basis set.[25a] Interaction energies were calculated using the full counterpoise correction method to account for the basis set superposition error (BSSE). For the most stable geometries, interaction energies were re-calculated using a very accurate CCSD(T)/CBS[26,27] level of theory by applying the double-triple (D, T) extrapolation scheme proposed by Helgaker and coworkers.[28] Energies of O–H···C interactions were calculated for model systems consisting of pyramidane and its derivatives and water molecules. Studied interactions involved the apical C atom of pyramidane (and its derivatives) and the hydrogen atom of a water molecule. Molecular electrostatic potentials (MEPs) were calculated and visualized using the Wave Function Analysis – Surface Analysis Suite (WFA–SAS) software.[29] Energy decomposition analysis (EDA) was done using the PSI4 software and the SAPT2/aug-cc-pVTZ level of theory.[30,31] All structures were visualized using Avogadro and Mercury programs.[32,33] The Cambridge Structural Database (CSD)[34] was searched using the ConQuest[35] software to find all square-pyramidal structures in which an apical carbon atom interacts with a hydrogen atom. The CSD was searched for all square-pyramidal structures with a carbon atom at the apex that is involved in a non-covalent contact with a hydrogen atom of another molecule. The distance between interacting C and H atoms was ≤ 2.9 Å (the sum of van der Waals radii for C and H), while the hydrogen atom positions were normalized.[36] The R factor was chosen to be < 0.05, and only non-disordered structures with 3D coordinates determined were considered for analysis. Hirshfeld maps were calculated using the Crystal Explorer software.[37] Hirshfeld surfaces for ZUQRUY and VIZMUN structures were calculated and mapped over d_{norm}. Non-covalent index (NCI) analysis was performed using Multiwfn and VMD programs at the MP2/aug-cc-pVTZ level, while the bond critical points were calculated and visualized in the Multiwfn program.[38–40] Natural bond orbital (NBO) analysis was performed at the MP2/cc-pVTZ level.[25b,41,42]

Results and discussion

Geometry optimizations and molecular electrostatic potential calculations

The optimized structures of pyramidane and its derivatives (Tables S1–S6, ESI†) are given in Fig. 2.

Vibrational frequencies were calculated, and the results showed no negative frequencies for any of the studied molecules, indicating that the optimized geometries represent true minima (see Fig. S1–S6 in the ESI†). Optimized geometries were used for MEP calculations. Calculated MEPs with the electrostatic potential values at the critical points above the apical carbon atoms are given in Fig. 3.

The results of molecular electrostatic potential calculations showed that in the case of all six pyramidal molecules, there is a strong negative electrostatic potential above the apical carbon atom. The strongest negative potential was detected in the case of the pyramidane molecule with four –CH$_3$ substituents

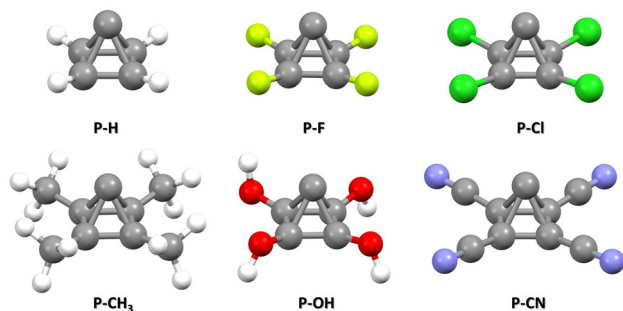**2564** | *Phys. Chem. Chem. Phys.*, 2025, **27**, 2563–2569

This journal is © the Owner Societies 2025

Fig. 2 Optimized geometries of a pyramidane molecule and its derivatives with −F, −Cl, −CH₃, −OH, and −CN substituents attached to four basal C atoms.

(P-CH₃) with the energy in the critical point of −48.76 kcal mol⁻¹. Quite strong negative potentials were also detected in pyramidane molecules substituted with four –OH groups (P-OH, −45.14 kcal mol⁻¹) and non-substituted pyramidane molecule (P-H, −45.06 kcal mol⁻¹). The least negative potential was calculated in the case of the pyramidane molecule with four –CN substituents (P-CN, −7.97 kcal mol⁻¹). For the structure containing the most negative critical point above the apical C atom (P-CH₃) natural population analysis (NPA) charges were calculated. The results confirmed the existence of a negative charge on the apical carbon atom (NPA charge in the C atom: −0.21). This is in agreement with previous results indicating that the electrostatic potential on the surface above the apical carbon atom may be negative. In a recent study by Pendás and coworkers, it was shown through ELF and QTAIM analysis that the apical carbon atom possesses a lone pair of electrons which generates the negative electrostatic potential around it.[43]

Interaction energy calculations

Interaction energies were calculated on model systems consisting of pyramidane or substituted pyramidane molecules and water molecules. One O–H fragment of the water molecule was orientated to form linear O–H···C interaction with the apical carbon atom of pyramidane or substituted pyramidane. The distance between interacting carbon and hydrogen atoms was varied, and interaction energies were calculated. Interaction energies calculated at the MP2/aug-cc-pVTZ level are given in Fig. 4.

The calculated energies of O–H···C interaction were in the interval from −7.40 to −2.05 kcal mol⁻¹. The strongest interaction (−7.40 kcal mol⁻¹) was found in the model system containing the P-CH₃ molecule. Very strong interaction was also found in the model system containing the unsubstituted pyramidane molecule, P-H (−6.41 kcal mol⁻¹). On the other hand, the weakest interaction was found in model system containing pyramidane molecule with CN substituents (P-CN, −2.05 kcal mol⁻¹). The geometries with optimal carbon–hydrogen distances are given in Fig. 5.

Analysis of the calculated hydrogen bond lengths is consistent with the results of interaction energies calculations and analysis of MEPs; the shortest hydrogen bonds (2.1 Å) are detected in the case of pyramidane molecules with the
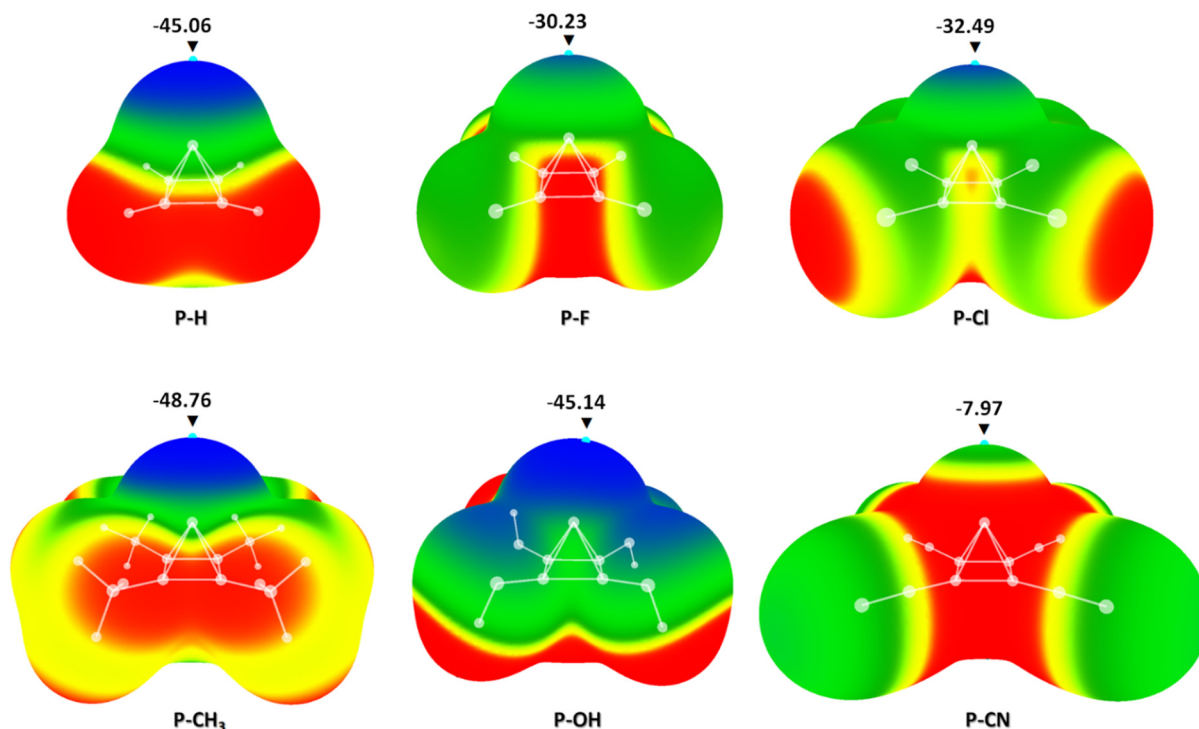

Fig. 3 Calculated electrostatic potential maps of a pyramidane molecule and its derivatives with −F, −Cl, −CH₃, −OH and −CN substituents attached to four basal C atoms. Values of energies in critical points are given in kcal mol⁻¹. Colour ranges, in kcal mol⁻¹, are: red, greater than 7.11; yellow, from 7.11 to 0.00; green, from −27.66 to 0.00; blue, more negative than −27.66. Blue dots refer to local minima on the molecular surfaces.
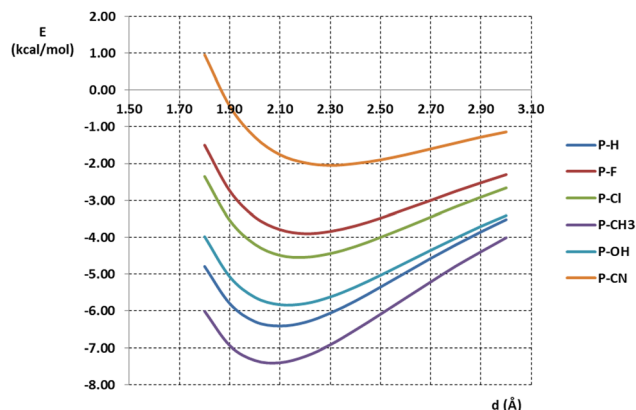
Fig. 4 Energies of O–H···C interactions between pyramidane or pyramidane derivatives and water molecule calculated at the MP2/aug-cc-pVTZ level of theory.

strongest interactions and the strongest negative electrostatic potential above the apical carbon atom (P-CH$_3$, P-OH, P-H). On the other hand, the longest O–H···C interaction was detected in the case of a hydrogen bond involving the P-CN molecule (the weakest interaction and the lowest negative potential value over the apical carbon atom). These findings are also consistent with the calculated energies of O–H···C interactions (Table 1). For the optimal geometries calculated at the MP2/aug-cc-pVTZ level, interaction energies were re-calculated using a very accurate CCSD(T)/CBS level of theory (Table 1).

The results showed that calculated interaction energies at the MP2/aug-cc-pVTZ level were in excellent agreement with the interaction energies calculated at the CCSD(T)/CBS level of theory. The strongest interaction calculated at the CCSD(T)/CBS level was found in the model system consisting of P-CH$_3$ molecule and water ($\Delta E_{\text{CCSD(T)/CBS}}$ = −7.43 kcal mol^{-1}). To better understand the nature of hydrogen bonding, the NBO analysis was performed on this model system. The results confirmed that electron transfer occurs from the lone pairs on the apical carbon atom to the antibonding orbital of the

Table 1 Energies of O–H···C interactions calculated at the CCSD(T)/CBS level

Model system	O–H···C distance (Å)	$\Delta E_{\text{CCSD(T)/CBS}}$ (kcal mol^{-1})
P-H	2.1	−6.41
P-F	2.2	−3.92
P-Cl	2.2	−4.58
P-CH$_3$	2.1	−7.43
P-OH	2.1	−5.87
P-CN	2.3	−2.00

hydrogen atom in the water molecule. Very strong interactions were also calculated in the case of model systems containing P-OH ($\Delta E_{\text{CCSD(T)/CBS}}$ = −5.87 kcal mol^{-1}) and P-H ($\Delta E_{\text{CCSD(T)/CBS}}$ = −6.41 kcal mol^{-1}) molecules. Moderately strong interactions were calculated in the case of P-F and P-Cl molecules as hydrogen atom acceptors (−3.92 and −4.58 kcal mol^{-1}, respectively). As expected, the weakest interaction was calculated for a model system containing the P-CN molecule ($\Delta E_{\text{CCSD(T)/CBS}}$ = −2.00 kcal mol^{-1}). These trends are generally consistent with the trends in the calculated values of the negative electrostatic potential above the apical carbon atom (Fig. 3), except for P-OH and P-H molecules. Interaction energies were also calculated at the MP2/aug-cc-pVTZ level without taking into account the Basis Set Superposition Error (BSSE) and the trends in energy values were not changed (Table S13, ESI†).

Hydrogen bond critical points were calculated at the MP2/aug-cc-pVTZ level and visualized (Fig. S7, ESI†), since it was shown that analysis of electron densities in these points can give deeper insight into the properties of hydrogen bonds.[44] Calculated values of electron density at bond critical points are in good correlation with calculated values of electrostatic potential at critical points above the apical carbon atom (Table S13, ESI†).

However, it is important to note that analysis of electrostatic potential maps could be used to explain only the contribution of electrostatics to the calculated interaction energies, while other contributions remain unknown. To reveal the role of other contributions to the total energy of the studied O–H···C interactions, we have performed an energy decomposition analysis.

Energy decomposition analysis

The energy decomposition analysis was performed using the SAPT2 method and the aug-cc-pVTZ level of theory. The results of the EDA calculations are given in Table 2.

The results of EDA calculations clearly indicate that the main energetic contribution to the O–H···C hydrogen bonds is the electrostatics. The strongest electrostatic contributions were calculated for model systems with the strongest interaction energies (P-CH$_3$, −10.64 kcal mol^{-1}, and P-H, −9.65 kcal mol^{-1}). Not surprisingly, the lowest contribution of the electrostatics was calculated for interaction involving the P-CN molecule, −2.66 kcal mol^{-1}. Besides electrostatics, contributions of induction and dispersion to the total energy of interaction are significant in all model systems. It could be noticed that the contribution of induction is stronger in the case of the P-H molecule than the P-OH molecule, which may be the reason why,
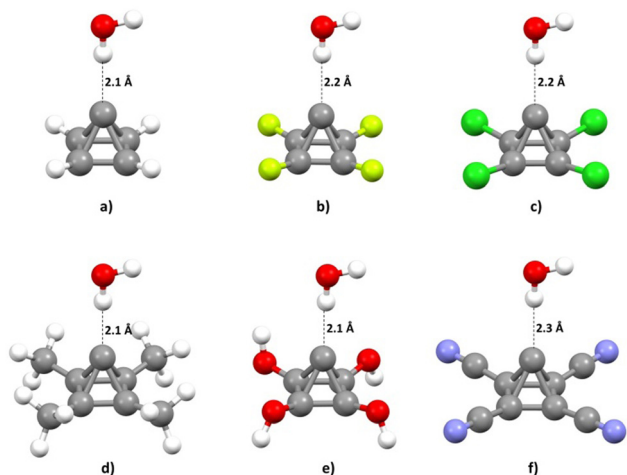

Fig. 5 Calculated optimal geometries (a–f) for studied model systems.

2566 | *Phys. Chem. Chem. Phys.*, 2025, **27**, 2563–2569

This journal is © the Owner Societies 2025

Table 2   The results of EDA calculations for the model systems shown in Fig. 2. Energies are given in kcal mol^{-1}

|	P-H	P-F	P-Cl	P-CH$_3$	P-OH	P-CN
Electrostatics	−9.65	−5.47	−6.01	−10.64	−8.72	−2.66
Exchange	10.02	6.30	6.53	10.80	9.61	4.11
Induction	−3.59	−2.15	−2.30	−4.01	−3.39	−1.32
Dispersion	−3.13	−2.51	−2.73	−3.52	−3.25	−2.14
Total SAPT	−6.35	−3.84	−4.50	−7.37	−5.75	−2.00
CCSD(T)/CBS	−6.41	−3.92	−4.58	−7.43	−5.87	−2.00

for these two systems, values of electrostatic potential in critical points are not consistent with the trends in calculated interaction energies. It is important to note that interaction energies calculated at the SAPT2/aug-cc-pVTZ level are in excellent agreement with CCSD(T)/CBS energies.

Analysis of crystal structures

Although neither pyramidane nor its derivatives studied in the frame of this research were synthesized and crystalized yet, analysis of possible carbon–hydrogen contacts in similar structures could be helpful for the prediction of the potential of the apical carbon atom in pyramidal molecules to form hydrogen bonds as hydrogen atom acceptors. Using the criteria defined in the Methodology section, the CSD was searched, and only two structures in which short carbon–hydrogen contacts exist were extracted (refcodes VIZMUN and ZUQRUY). Three-dimensional representations of these structures are given in
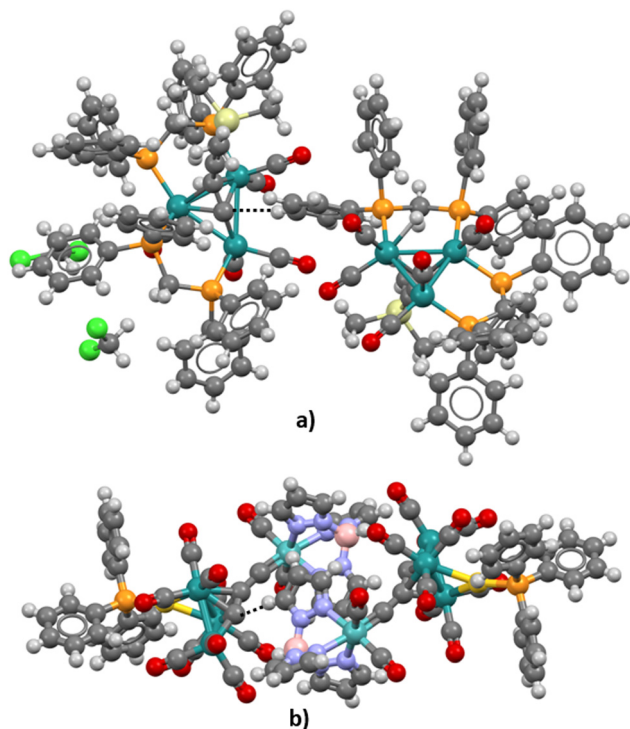
Fig. 6   The fragment of (a) ZUQRUY and (b) VIZMUN structures with short contacts (dashed line) between apical carbon atoms and hydrogen atoms from another molecule. The carbon–hydrogen distances are $d = 2.74$ Å in ZUQRUY and $d = 2.80$ Å in the VIZMUN structure.
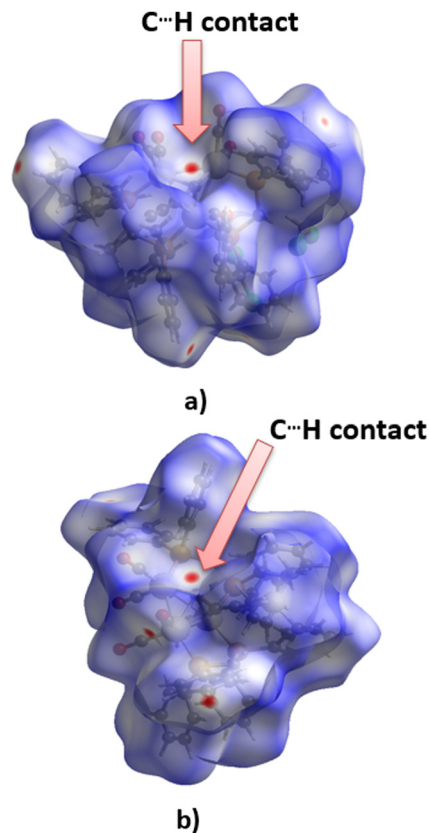
Fig. 7   Hirshfeld surfaces (d_{norm}) calculated for fragments of (a) ZUQRUY and (b) VIZMUN structures. The red area on the surface above the apical carbon atoms indicates the existence of C···H contacts.

Fig. 6. Both structures contain Ru heteroatoms connected to an apical carbon atom.

In the case of the ZUQRUY structure, the distance between the apical carbon atom of the pyramidal fragment and the hydrogen atom of the C–H fragment is 2.74 Å, which is significantly shorter than the sum of van der Waals radii for C and H atoms (2.9 Å). Also, the angle defined by C–H···C atoms is 175.08°, indicating the presence of a directional interaction, which is usual in the case of strong hydrogen bonds. A similar situation was noticed in the VIZMUN structure (the distance between C and H atoms was measured to be 2.80 Å, while the angle defined by C–H···C atoms is 156.66°). Although the comparison between the measured distance between two atoms and the sum of van der Waals radii is not definite proof of the existence of non-covalent contacts, it is a good indicator of possible C–H···C interactions.

The tendency of apical carbon atoms to form non-covalent contacts with hydrogen atoms in these structures is evident from the analysis of Hirsfeld surfaces for ZUQRUY and VIZMUN structures (Fig. 7). Red regions above the apical carbon atoms on the Hirsfeld surfaces for both ZUQRUY and VIZMUN structures indicate the existence of C–H···C interactions between C–H fragments and apical carbon atoms.

To confirm the existence of C–H···C interactions in these crystal structures, non-covalent index analysis was performed.

This journal is © the Owner Societies 2025

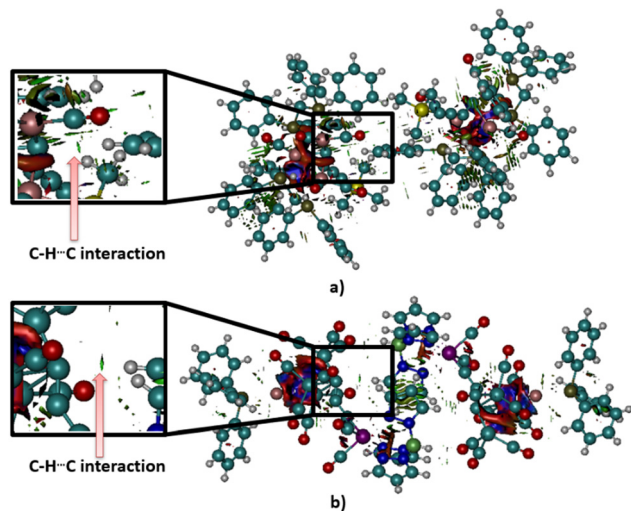*Phys. Chem. Chem. Phys.*, 2025, **27**, 2563–2569 | **2567**

Fig. 8 Calculated NCI plots for (a) ZUQRUY and (b) VIZMUN structures. Green surfaces correspond to the attractive regions of non-covalent interactions (the isosurface value was selected to be 0.5, while the interval of the color range is from −0.035 to 0.2).

The calculated NCI plots are given in Fig. 8. Results of the analysis of NCI plots showed that in the case of the ZUQRUY structure (Fig. 8a), there is an area of non-covalent bonding between an apical carbon atom and a hydrogen atom from the neighbouring C–H fragment (green area). Similar results were obtained in the case of the VIZMUN structure (Fig. 8b). The green area between the apical carbon atom and a hydrogen atom of the C–H fragment in the VIZMUN structure also indicates the existence of an attractive non-covalent contact.

Conclusions

In this work, high-level quantum chemical calculations were combined with the analysis of available crystal structures to predict the properties of hydrogen bonds involving apical pyramidane carbon atoms as hydrogen acceptors. Six structures, including pyramidane (P-H) and its derivatives with four substituents on basal carbon atoms (P-F, P-Cl, P-CH$_3$, P-OH, P-CN), were considered within this study. The results of the analysis of molecular electrostatic potentials showed that there is an area of negative electrostatic potential above the apical carbon atom in all six examined structures. The strongest negative potential was detected above the apical carbon atom of the P-CH$_3$ structure (−48.76 kcal mol^{-1}), while the very strong negative potential was detected in the case of P-OH (−45.14 kcal mol^{-1}) and P-H (−45.06) molecules, too. The weakest negative potential was calculated above the apical carbon atom of the P-CN structure (−7.97 kcal mol^{-1}). Since these results indicated that apical carbon atoms might act as hydrogen atom acceptors in hydrogen bonds, six model systems containing already mentioned pyramidal molecules and water molecules were made, and interaction energies were calculated. The results of interaction energy calculations showed that studied O–H···C interactions can be quite strong,

up to $\Delta E_{\text{CCSD(T)/CBS}} = -7.43$ kcal mol^{-1} in the case of P-CH$_3$ molecule as a hydrogen atom acceptor. The weakest hydrogen bond was calculated in the case of a model system containing a P-CN molecule (−2.00 kcal mol^{-1}). This agrees with the results of electrostatic potential calculations, indicating that these interactions are mainly electrostatic. Energy decomposition analysis was performed on all model systems, and the results confirmed that all studied interactions are indeed primarily electrostatic, with strong contributions from induction and dispersion. Although the studied molecules have not yet been synthesized, crystal structures of similar pyramidal molecules with apical carbon atoms involved in hydrogen bonds were found in the Cambridge Structural Database.

The results presented in this study are in agreement with previous results showing that increased electron density is present at the apex of pyramidane-like molecules. To the best of our knowledge, this is the first study of the energies of hydrogen bonds involving apex pyramidane carbon as a hydrogen atom acceptor. The results obtained within this study may be of great importance for understanding the non-covalent bonding patterns in the case of hydrogen bonds involving pyramidal-shaped molecules.

Data availability

The data supporting this article have been included as part of the ESI.†

Conflicts of interest

There are no conflicts to declare.

Acknowledgements

Notes and references

1 T. Wang, Y. Zhang, B. Huang, B. Cai, R. R. Rao, L. Giordano, S.-G. Sun and Y. Shao-Horn, *Nat Catal.*, 2021, **4**, 753.
2 R.-B. Lin, Y. He, P. Li, H. Wang, W. Zhou and B. Chen, *Chem. Soc. Rev.*, 2019, **48**, 1362.
3 B. Dereka, Q. Yu, N. H. C. Lewis, W. B. Carpenter, J. M. Bowman and A. Tokmakoff, *Science*, 2021, **371**, 160.
4 P. A. Song and H. Wang, *Adv. Mater.*, 2020, **32**, 1901244.
5 G. R. Desiraju, *Angew. Chem., Int. Ed.*, 2011, **50**, 52.
6 B. Wang, R.-B. Lin, Z. Zhang, S. Xiang and B. Chen, *J. Am. Chem. Soc.*, 2020, **142**, 14399.
7 M. Nishio, Y. Umezawa, J. Fantini, M. S. Weissd and P. Chakrabartie, *Phys. Chem. Chem. Phys.*, 2014, **16**, 12648.
8 J. Ran and P. Hobza, *J. Phys. Chem. B*, 2009, **113**(9), 2933.

2568 | *Phys. Chem. Chem. Phys.*, 2025, **27**, 2563–2569

This journal is © the Owner Societies 2025

9 D. S. Kretić, D. I. Radovanović and D. Ž. Veljković, *Phys. Chem. Chem. Phys.*, 2021, **23**, 7472.

10 E. Arunan, G. R. Desiraju, R. A. Klein, J. Sadlej, S. Scheiner, I. Alkorta, D. C. Clary, R. H. Crabtree, J. J. Dannenberg, P. Hobza, H. G. Kjaergaard, A. C. Legon, B. Mennucci and D. J. Nesbitt, *Pure Appl. Chem.*, 2011, **83**, 1637.

11 S. Grabowski, *Chem. Commun.*, 2024, **60**, 6239.

12 A. J. Arduengo, III, S. F. Gamper, M. Tamm, J. C. Calabrese, F. Davidson and H. A. Craig, *J. Am. Chem. Soc.*, 1995, **117**, 572.

13 M. Jabłoński and M. Palusiak, *Phys. Chem. Chem. Phys.*, 2009, **11**, 5711.

14 S. J. Grabowski, *CrystEngComm*, 2023, **25**, 4550.

15 O. Loveday and J. Echeverría, *Cryst. Growth Des.*, 2021, **21**, 5961.

16 V. Y. Lee, Y. Ito, A. Sekiguchi, H. Gornitzka, O. A. Gapurenko, V. I. Minkin and R. M. Minyaev, *J. Am. Chem. Soc.*, 2013, **135**, 8794.

17 Q. Sun, C. G. Daniliuc, X. Yu, C. Mück-Lichtenfeld, G. Kehr and G. Erker, *J. Am. Chem. Soc.*, 2022, **144**, 7815.

18 V. Y. Lee, H. Sugasawa, O. A. Gapurenko, R. M. Minyaev, V. I. Minkin, H. Gornitzka and A. Sekiguchi, *Chem. – Eur. J.*, 2016, **22**, 17585.

19 V. Y. Lee, Y. Ito, O. A. Gapurenko, A. Sekiguchi, V. I. Minkin, R. M. Minyaev and H. Gornitzka, *Angew. Chem., Int. Ed.*, 2015, **54**, 5654.

20 Y. Canac and G. Bertrand, *Angew. Chem., Int. Ed.*, 2003, **42**, 3578.

21 V. Y. Lee, O. A. Gapurenko, Y. Ito, T. Meguro, H. Sugasawa, A. Sekiguchi, R. M. Minyaev, V. I. Minkin, R. H. Herber and H. Gornitzka, *Organometallics*, 2016, **35**, 346.

22 F. Ren, D. Cao, W. Shi and H. Gao, *J. Mol. Model.*, 2016, **22**, 97.

23 M. J. Frisch, G. W. Trucks, H. B. Schlegel, G. E. Scuseria, M. A. Robb, J. R. Cheeseman, G. Scalmani, V. Barone, B. Mennucci, G. A. Petersson, H. Nakatsuji, M. Caricato, X. Li, H. P. Hratchian, A. F. Izmaylov, J. Bloino, G. Zheng, J. L. Sonnenberg, M. Hada, M. Ehara, K. Toyota, R. Fukuda, J. Hasegawa, M. Ishida, T. Nakajima, Y. Honda, O. Kitao, H. Nakai, T. Vreven, J. A. Montgomery Jr., J. E. Peralta, F. Ogliaro, M. Bearpark, J. J. Heyd, E. Brothers, K. N. Kudin, V. N. Staroverov, R. Kobayashi, J. Normand, K. Raghavachari, A. Rendell, J. C. Burant, S. S. Iyengar, J. Tomasi, M. Cossi, N. Rega, J. M. Millam, M. Klene, C. Adamo, R. Cammi, J. W. Ochterski, R. L. Martin, K. Morokuma, V. G. Zakrzewski, G. A. Voth, P. Salvador, J. J. Dannenberg, S. Dapprich, A. D. Daniels, Ö. Farkas, J. B. Foresman, J. V. Ortiz, J. Cioslowski and D. J. Fox, *Gaussian 09, Revision D.01*, Gaussian, Inc., Wallingford CT, 2013.

24 C. Møller and M. S. Plesset, *Phys. Rev.*, 1934, **46**, 618.

25 (*a*) R. A. Kendall, T. H. Dunning and R. J. Harrison, *J. Chem. Phys.*, 1992, **96**, 6796; (*b*) T. H. Dunning Jr., *J. Chem. Phys.*, 1989, **90**, 1007.

26 K. Raghavachari, G. W. Trucks, J. A. Pople and M. A. Head-Gordon, *Chem. Phys. Lett.*, 1989, **157**, 479.

27 M. O. Sinnokrot and C. D. Sherrill, *J. Phys. Chem. A*, 2004, **108**, 10200.

28 (*a*) T. Helgaker, W. Klopper, H. Koch and J. Noga, *J. Chem. Phys.*, 1997, **106**, 9639; (*b*) A. Halkier, T. Helgaker, P. Jørgensen, W. Klopper, H. Koch, J. Olsen and A. K. Wilson, *Chem. Phys. Lett.*, 1998, **286**, 243; (*c*) A. Halkier, T. Helgaker, P. Jørgensen, W. Klopper and J. Olsen, *Chem. Phys. Lett.*, 1999, **302**, 437; (*d*) D. Feller, *J. Chem. Phys.*, 1992, **96**, 6104.

29 F. A. Bulat, A. Toro-Labbé, T. Brinck, J. S. Murray and P. Politzer, *J. Mol. Model.*, 2010, **16**, 1679.

30 R. M. Parrish, L. A. Burns, D. G. A. Smith, A. S. Simmonett, A. E. DePrince, E. G. Hohenstein, U. Bozkaya, A. Y. Sokolov, R. Di Remigio, R. M. Richard, J. F. Gonthier, A. M. James, H. R. McAlexander, A. Kumar, M. Saitow, X. Wang, B. P. Pritchard, P. Verma, H. F. Schaefer, K. Patkowski, R. A. King, E. F. Valeev, F. A. Evangelista, J. M. Turney, T. D. Crawford and C. D. Sherrill, *J. Chem. Theory Comput.*, 2017, **13**, 3185.

31 E. G. Hohenstein and C. D. Sherrill, *J. Chem. Phys.*, 2010, **133**, 014101.

32 M. D. Hanwell, D. E. Curtis, D. C. Lonie, T. Vandermeersch, E. Zurek and G. R. Hutchison, *J. Cheminform.*, 2012, **4**, 17.

33 C. F. Macrae, I. J. Bruno, J. A. Chisholm, P. R. Edgington, P. McCabe, E. Pidcock, L. Rodriguez-Monge, R. Taylor, J. van de Streek and P. A. Wood, *J. Appl. Cryst.*, 2008, **41**, 466.

34 F. H. Allen, *Acta Crystallogr., Sect. B: Struct. Sci.*, 2002, **58**, 380; C. R. Groom, I. J. Bruno, M. P. Lightfoot and S. C. Ward, *Acta Crystallogr., Sect. B: Struct. Sci.*, 2016, **72**, 171.

35 I. J. Bruno, J. C. Cole, P. R. Edgington, M. Kessler, C. F. Macrae, P. McCabe, J. Pearson and R. Taylor, *Acta Crystallogr., Sect. B: Struct. Sci.*, 2002, **58**, 389.

36 A. Bondi, *J. Phys. Chem.*, 1964, **68**, 441.

37 P. R. Spackman, M. J. Turner, J. J. McKinnon, S. K. Wolff, D. J. Grimwood, D. Jayatilaka and M. A. Spackman, *J. Appl. Crystallogr.*, 2021, **54**, 1006.

38 T. Lu and F. Chen, *J. Comput. Chem.*, 2012, **33**, 580.

39 E. R. Johnson, S. Keinan, P. Mori-Sánchez, J. Contreras García, A. J. Cohen and W. Yang, *J. Am. Chem. Soc.*, 2010, **132**, 6498.

40 W. Humphrey, A. Dalke and K. Schulten, *J. Mol. Graphics*, 1996, **14**, 33.

41 A. E. Reed, L. A. Curtiss and F. Weinhold, *Chem. Rev.*, 1988, **88**, 899.

42 F. Weinhold and C. R. Landis, *Valency and Bonding: A Natural Bond Orbital Donor-Acceptor Perspective*, Cambridge University Press, Cambridge, 2005.

43 L. Vidal, D. Barrena-Espés, J. Echeverría, J. Munárriz and Á. M. Pendás, *ChemPhysChem*, 2024, **25**, e202400329.

44 L. Soriano-Agueda, *Int. J. Quantum Chem.*, 2024, **124**, e27352.

This journal is © the Owner Societies 2025

Phys. Chem. Chem. Phys., 2025, **27**, 2563–2569 | **2569**